Geobios

A spatangoid echinoid assemblage from the Gutingkeng Formation (Early Pleistocene) of Taiwan and its paleoenvironmental and geological implications

--Manuscript Draft--

Manuscript Number:	GEOBIO-D-23-00076R3
Article Type:	Research paper
Keywords:	Echinodermata; Echinoidea; Quaternary biostratigraphy; paleoenvironment; orogeny
Corresponding Author:	Chien-Hsiang Lin Biodiversity Research Center Academia Sinica Taipei, None Selected TAIWAN
First Author:	Chia-Hsin Hsu
Order of Authors:	Chia-Hsin Hsu
	Jih-Pai Lin
	Chien-Hsiang Lin
Abstract:	Heart urchins (Echinoidea: Spatangoida) collectively represent a highly diverse group of echinoids with abundant global fossil and extant records. Despite their wide distribution, the preservation challenges associated with their delicate and thin tests have led to limited comprehensive studies of this fossil group in Taiwan. Here, we report a new spatangoid echinoid assemblage from the Gutingkeng Formation (Early Pleistocene). Despite the inherent fragility and pronounced deformations in the studied specimens, the preserved key diagnostic characteristics (pore pairs in ambulacrum III and oral plating) indicate most of the fossil echinoids belong to genera Schizaster and Brissopsis. Moreover, based on detailed taphonomic and functional morphological examination, the paleoenvironment of the assemblage is interpreted as a low-energy, fine-grained soft substrate in a deeper shallow-water setting. Furthermore, this assemblage shares a high similarity with Assemblage 3 at the S'Archittu-Cajaragas section in the Miocene of Sardinia, supporting the notion that echinoids are excellent paleoenvironmental indicators, as similar echinoid faunas can be found across continents when environmental conditions are similar. On the other hand, the temporal and geographical distribution of Schizaster-rich echinoid assemblages in Taiwan may be correlated with the Cenozoic orogeny history of Taiwan.
Suggested Reviewers:	James Nebelsick nebelsick@uni-tuebingen.de
	Andrea Mancosu andrea.mancosu@gmail.com
	Tobias Grun tgrun@ufl.edu
	Mike Reich mike.reich@lmu.de
Response to Reviewers:	Point-by-point comments and responses --- Manuscript Number: GEOBIO-D-23-00076R2 A spatangoid echinoid assemblage from the Gutingkeng Formation (Early Pleistocene) of Taiwan and its paleoenvironmental and geological implications Editor in Chief: Two reviewers (already solicited in the previous rounds of peer review) as well as Geobios Associate-Editor Dr. Bertrand Lefebvre and I have now carefully looked at the second revised version of the manuscript you submitted for publication in Geobios – see comments below as well as the three attached files uploaded by rev. #4. I agree with them that your manuscript has been now very significantly improved with respect

Cover

Accepted MS OK for Production.

A spatangoid echinoid assemblage from the Gutingkeng Formation (Early Pleistocene) of Taiwan and its paleoenvironmental and geological implications ✡

Chia-Hsin Hsu [a], Jih-Pai Lin [a,*], Chien-Hsiang Lin [b,*]

[a] Department of Geosciences, National Taiwan University, Taipei, Taiwan

[b] Biodiversity Research Center, Academia Sinica, Taipei, Taiwan

[*] Corresponding authors. E-mail addresses: alexjplin@ntu.edu.tw (J.-P. Lin), chlin.otolith@gmail.com (C.-H. Lin).

✡ Corresponding editor: Bertrand Lefebvre.

Abstract

Heart urchins (Echinoidea: Spatangoida) collectively represent a highly diverse group of echinoids with abundant global fossil and extant records. Despite their wide distribution, the preservation challenges associated with their delicate and thin tests have led to limited comprehensive studies of this fossil group in Taiwan. Here, we report a new spatangoid echinoid assemblage from the Gutingkeng Formation (Early Pleistocene). Despite the inherent fragility and pronounced deformations in the studied specimens, the preserved key diagnostic characteristics (pore pairs in ambulacrum III and oral plating) indicate most of the fossil echinoids belong to genera *Schizaster* and *Brissopsis*. Moreover, based on detailed taphonomic and functional morphological examination, the paleoenvironment of the assemblage is interpreted as a low-energy, fine-grained soft substrate in a deeper shallow-water setting. Furthermore, this assemblage shares a high similarity with Assemblage 3 at the S'Archittu-Cajaragas section in the Miocene of Sardinia, supporting the notion that echinoids are excellent paleoenvironmental indicators, as similar echinoid faunas can be found across continents when environmental conditions are similar. On the other hand, the temporal and geographical distribution of *Schizaster*-rich echinoid

assemblages in Taiwan may be correlated with the Cenozoic orogeny history of Taiwan.

Keyword:
Echinodermata
Echinoidea
Quaternary biostratigraphy
Paleoenvironment
Orogeny

1. Introduction

Irregular echinoids are a prominently documented group of echinoderms in the Cenozoic era, as evidenced by numerous studies (Sprinkle, 1980; Pereira, 2015; Mondiardino Koch and Thompson, 2020). Currently, the infraclass Irregularia Latreille, 1825 encompasses around 400 recognized genera (Kroh and Smith, 2010). The radiation of irregular echinoids is believed to be closely associated with a range of morphological innovations (Hopkins and Smith, 2015; Boivin et al., 2018), enabling their successful colonization in various habitats. The close relationship between irregular echinoids and their surrounding environment has established some of them as reliable environmental indicators, both in the present and through their fossils. So far, numerous studies have utilized irregular echinoids as essential tools for understanding past environments (Néraudeau et al., 2001; Kroh, 2003b; Kroh and Nebelsick, 2003; Mancosu and Nebelsick, 2016, 2019). Examining the Cenozoic fossil record of irregular echinoids provides invaluable insights into environmental changes in the past. Additionally, it serves as an excellent case study illustrating how animals adapt to new environments to expand their habitats.

Taiwan plays a significant role in advancing our understanding of the Cenozoic radiation of irregular echinoids in the northwestern Pacific, as highlighted in a recent study by Lee et al. (2023). This study investigated the phylogenetic relationships of 25 taxa, belonging to eleven luminacean families and proposed three new superfamilies, including Astriclypeoidea Lin in Lee et al., 2023, Mellitoidea Lin in Lee et al., 2023, and Taiwanasteroidea Lin in Lee et al., 2023, instead of the currently recognized superfamily Scutelloidea Gray, 1825. As a result, Lee et al. (2023)

interpreted the tropical eastern Indian and western Pacific Ocean (EIWP) as key biodiversity and migration centers for shallow marine echinoids. Significantly, the waters adjacent to Taiwan have emerged as a major crossroad for the migration of luminacean taxa and related irregular echinoids. Therefore, the study of fossil echinoid records in Taiwan is important to understand the dynamic of hypothesized migration routes through time.

The studies of fossil echinoids in Taiwan initiated in the middle of the 20th century. The diligent efforts of researchers, including Hayasaka (Hayasaka and Morishita, 1947a, 1947b; Hayasaka, 1948a, 1948b), Wang (Cheng and Wang, 1981; Wang, 1984a, 1984b, 1985, 1986), and more recent contributors (Lin et al., 2021b; Ho et al., 2022), have resulted in extensive studies based on the abundant echinoid fossils in Taiwan. For spatangoid echinoid assemblages, *Schizaster*-rich echinoid assemblages have been reported from the Oligocene Slate Belt in Taiwan (Tokunaga, 1903; Nisiyama, 1933; Hayasaka, 1948b), co-occurring with the less abundant *Brissopsis* species (Nisiyama, 1968). Chuang (2020) reported a *Faorina*-dominated echinoid assemblage from the Lower Pleistocene Yujing Shale in southern Taiwan, with the co-occurrences of the species of genera *Maretia*, *Schizaster* (*Ova*), *Breynia*, *Brissus*, and *Moira*. Kuo (2023) reported an *Echinocardium*-dominated echinoid assemblage from the Pleistocene Chiting Fm. Recently, Chen et al. (in press) reported and analyzed comprehensively the spatangoid echinoid assemblage, which is dominated by the species of genera *Moira* and *Breynia*, from the Middle Miocene Nangang Fm. at NE Taiwan, with the co-occurrences of *Faorina* and *Schizaster*. In this study, we report a new spatangoid echinoid assemblage dominated by the species of genera *Schizaster* and *Brissopsis*. We provide a comprehensive discussion on the ecological and geological implications of this new occurrence.

2. Geological setting

Fossil specimens were collected from an outcrop located adjacent to a tributary of the Erren River in Tianliao District, Kaohsiung City (Fig. 1; GPS coordinates: 22°53’38.3’’N, 120°23’16.0’’E). Outcrop consists of massive mudstone with no obvious bioturbation. The outcrop represents a portion of the Gutingkeng Fm., characterized by thick mudstone layers, which exceed 4000 m in thickness (Chen, 2016). The Gutingkeng Fm. is widely distributed throughout the foothills of southern

Taiwan (Hu and Tao, 1982; Chen, 2016). However, due to the prevalence of poorly cemented mudstone within this formation, the areas covered by this formation often endure substantial erosional processes, resulting in the creation of a badland landscape (Fig. 2(A)). Based on extensive nannofossil biostratigraphy and magnetostratigraphy research conducted within the study area, the entire Gutingkeng Fm. is estimated to be deposited between 5.6 and 0.78 Ma (Horng and Shea, 1994; Shea and Horng, 1999). Moreover, the studied outcrop can be correlated further within the small *Gephyrocapsa* Zone (1.24-1.03 Ma) based on nannofossils reported in Shea and Horng (1999) (Fig. 1(C)). In terms of sedimentary environment, the Gutingkeng Fm. exhibits a gradual shallowing trend from the base to the top, with the majority of the sediments deposited in a middle offshore setting (Wang, 1992; Chen, 2016).

Fossils from the Gutingkeng Fm. have not received extensive documentation in the literature. Most studies have predominantly focused on microfossils, including foraminiferans and ostracods (Hu and Tao, 1982, 1986). Notably, from the lower part of the Gutingkeng Fm., Hu and Tao (1982) reported a new species of solitary coral *Caryophyllia* (*Acanthocyathus*) *chaochii* Hu and Tao, 1982, while Wang (1984b) reported a new species of tiny sand dollar now recognized as *Sinaechinocyamus gutingkengensis* (Wang, 1984). In the upper part of the Gutingkeng Fm., the Fengshan Reservoir in Kaohsiung City stands out as one of the extensively studied regions. It has yielded records of at least 53 species of bryozoans and 81 species of mollusks (Hu, 1987; Hu and Tao, 1992). More recently, Lin et al. (2021a) mentioned the presence of fossil fish from the Gutingkeng Fm., and Lin et al. (2023) reported an extensive collection of fish otoliths from the Early Pliocene part of the formation, documenting the presence of 64 fish taxa.

3. Material and methods

The fossil echinoids examined in this study, located in Tiaoliao, Kaohsiung, were initially discovered during sediment sampling for fish otolith fossils in the summer of 2023. Fossil echinoids were frequently observed on the surface of the strata exposed on the outcrop (Fig. 2(B)). However, due to the delicate nature of these echinoid specimens, multiple sampling activities were subsequently conducted to acquire higher-quality specimens. The studied specimens were extracted using a hammer and chisel and were then meticulously cleaned using steel needle files. Water was

intentionally avoided during this cleaning process to prevent damage and to effectively remove the surrounding sediments. Standard morphological terms (Lewis and Donovan, 2007) are adopted for description (Fig. 3), and fossil specimens are compared to the extant species in Taiwan. Oral plating figures are illustrated based on the remaining tests and the line of the suture on the specimens. In total, 67 specimens from the spatangoid echinoid assemblage of the Gutingkeng Fm. were examined and included in this study. In short, 13 specimens were identified as belonging to the genus *Schizaster* (Fig. 4), 16 specimens were identified as belonging to the genus *Brissopsis* (Fig. 5), and the remainder are fossil spatangoids that remain to be identified. All figured specimens are stored in the Biodiversity Research Museum, Academia Sinica, Taiwan (BRMAS) under the registration number ASIZF.

4. Systematic paleontology

Phylum Echinodermata Bruguière, 1791
Sub-phylum Echinozoa von Zittel, 1895
Class Echinoidea Schumacher, 1817
Order Spatangoida Agassiz, 1840
Family Schizasteridae Lambert, 1905
Genus ***Schizaster*** Agassiz, 1836

Diagnosis (modified from Mortensen, 1951; Kroh, 2005; Smith and Kroh, 2011)**:** Test heart-shaped, with deep frontal notch. Apical system with 2, 3 or 4 genital pores (see remarks). Ambulacrum III moderately to deeply sunken aborally, densely crowded, with single or double series pore pairs. Petals moderately to deeply sunken aborally, elongated tear-shaped, flexed inwards. Anterior petals significantly longer and more flexed than posterior petals. Petal tips slightly flexed. Labrum short and wide, not extending beyond first ambulacral plate, broad between labrum and sternal plates. Sternal plates elongated, nearly reach posterior margin. Plastron mesamphisternous, with large and symmetric sternal plates and biserially offset episternal plates.

Remarks: The classification of the genera *Schizaster*, *Paraster*, and *Ova* has been a subject of debate for decades. Mortensen (1951) differentiated between *Schizaster* and *Paraster* based on the number of genital pores, attributing two to *Schizaster* and four to *Paraster*. He also regarded *Ova* as a subgenus of *Schizaster*, distinguishing it

from *Schizaster* by the irregularly arranged double series pore pairs in ambulacrum III of *Ova* (Mortensen, 1951). Therefore, in Mortensen's classification scheme, *Schizaster*, *Paraster*, and *Ova* were characterized by having 2, 4, and 2 genital pores, respectively. Furthermore, for pore pairs in ambulacrum III, *Schizaster*, *Paraster*, and *Ova* were categorized into regular single, regular single, and irregular double series, respectively.

The Echinoid Directory (Smith and Kroh, 2011) illustrated a well-preserved specimen of *Schizaster studeri* (the type species of the genus *Schizaster*) from the type locality that exhibits four genital pores. This observation led to the redefinition of the genus *Schizaster* as a taxon characterized by the presence of four genital pores. Consequently, both *Schizaster* and *Paraster* possess four genital pores and exhibit regular single series pore pairs in ambulacrum III, resulting in synonymizing these two genera. Schultz (2009) therefore suggested a revised classification, placing species with four genital pores within *Schizaster* and those with only two genital pores in *Ova*. However, it is important to note that this revision has not been universally adopted, and the World Echinoidea Database (Kroh and Mooi, 2023) has not implemented this change into its classification scheme. Therefore, we have primarily followed Mortensen's classification, disregarding genital pore numbers and synonymizing *Paraster* with *Schizaster*, which is consistent with the prevailing classification of schizasteroid echinoids (Kroh, 2005; Filander and Griffiths, 2017). Additionally, a detailed ontogenetic study by McNamara (1995) revealed that genital pore numbers can vary at different stages of ontogeny within a single *Schizaster* species, providing further support for the classification approach.

Schizaster sp.

Figs. 4, 6(A–C), 7

Material: 13 specimens (ASIZF0100704, ASIZF0100810 to ASIZF0100814, and ASIZF0100820 to ASIZF0100826; Table S1, Appendix A).

Occurrence: Tianliao, Kaohsiung. Gutingkeng Fm., Early Pleistocene.

Description: Test small (mostly <4 cm in length), heart shaped (Figs. 4(B), 6(A)), widest point slightly closer to anterior margin (Figs. 4(B), 6(A)), moderately convex at posterior (Fig. 4(F)). Aboral surface slope toward anterior margin (Fig. 4(F)), greatest height on posterior keel; slightly narrow, moderately depressed ambulacrum III extending to oral surface at anterior end; pore pairs regularly arranged in single

series (Figs. 4(A, E), 6(B, C)). Apical system slightly near to posterior margin (Figs. 4(B, E), 6(A, C)), genital pores not obvious. Petals moderately depressed. Anterior petals elongated tear shaped, flexed inwards, three times longer than posterior petals (Figs. 4(A, B, E), 6(A–C)). Petal tips slightly flexed outwards (Figs. 4(G, H), 6(A, B)). Numbers of pore pairs about 20 to 25 in ambulacrum II, III, and IV; 10 to 15 in posterior petals (Figs. 4(A, E), 6(B, C)). Oral surface slightly convex, ambulacrum slightly depressed (Fig. 4(H)). Peristome near anterior margin (Fig. 4(H, I)). Plastron slightly inflated, ovate, greatest width very close to posterior margin (Figs. 4(G, H), 6(A, B)). Periproct at posterior keel end, closer to greatest height (Fig. 4(D)). Peripetalous and lateroanal fasciole not obvious. Labrum short and wide, reaching half of first ambulacral plate, broad between labrum and sternal plates (Figs. 4(H), 7(A)). Sternal plates elongated, nearly reaching posterior margin, the suture with episternal plates near posterior margin (Figs. 4(G–I), 7). Episternal plates flattened hexagonal. Plastron mesamphisternous, with symmetric sternal plates and biserially offset episternal plates (Figs. 4(H), 7(A)).

Remarks: Despite the fragility of these specimens attributed to their thin tests and susceptibility to dissolution in meteoric water, their taxonomic status can be revealed due to the preservation of key diagnostic characteristics. Notably, critical diagnostic features such as fascioles and genital pores, were unfortunately not preserved on the studied specimens. However, their ambulacrum III being sunken, paired ambulacra petaloid with the posterior pair obviously shorter than the anterior, sunken labrum being short and T-shaped and not extending beyond the start of the second ambulacral plate, and flattened hexagonal episternal plates suggest that they likely belong to the family Schizasteridae (Mortensen, 1951; Smith and Kroh, 2011). Despite the overall similarity in outline with some species of Hemiasteridae, hemiasteroids can be easily excluded because of their longitudinally elongate labrum that mostly extends beyond the start of the second ambulacral plate.

Additionally, the densely crowded single series pore pairs in ambulacrum III, elongated tear-shaped petals that are flexed inwards, anterior petals that are significantly longer and more flexed than posterior petals, elongated sternal plates that nearly reach the posterior margin, and the mesamphisternous plastron further supports the classification of these specimens within the genus *Schizaster* (Mortensen, 1951; McNamara, 1995). Although most of the studied specimens exhibit several features that are not typical of most *Schizaster* species, including a

shallow frontal notch, narrow ambulacrum III, and a smaller petaloid area, these features are likely not original characteristics but rather the result of compaction and deformation. When subjected to lateral stress, the concave ambulacrum, being the weakest plate boundary of the test, may suffer the most severe damage (Fig. 5(C)), potentially causing the width of the ambulacrum to be underestimated. When subjected to normal stress perpendicular to the oral or aboral surface, the spatangoid test may become flattened. Consequently, the lateral test will spread out at the oral and aboral margins in front view, making the petaloid area appear small due to visual bias. In summary, rather than relying on potentially biased features, we place greater confidence in features that are more stable, such as pore pairs and oral plating.

When comparing the studied fossil specimens to extant *Schizaster* species found in Taiwan, it is evident that the studied specimens are relatively smaller in size. It remains uncertain whether this size difference is due to individual variation or if it represents a distinct species. The studied specimens obviously differ from *Schizaster* (*Ova*) *lacunosus*, one of the most common extant schizasteroids in Taiwanese waters, as they exhibit a much wider sunken aboral ambulacrum III and a deeper frontal notch. Another notable difference is that *Schizaster* (*Ova*) *lacunosus* has distinctly flexed petals, with the tips bent outwards, whereas the petal tips of the studied specimens are only slightly bent outwards (Figs. 4(A, B), 6(A, B)). In comparison to another recorded extant schizasteroid species in Taiwan, *Schizaster compactus*, the studied specimens also possess a much wider sunken aboral ambulacrum III and a deeper frontal notch, although those of *S. compactus* are obviously shallower and narrower than those of *S. lacunosus*. We conclude that the studied specimens do not belong to any extant schizasteroid species found in Taiwanese waters.

Family Brissidae Gray, 1855
Subfamily Brissopsinae Lambert, 1905
Genus ***Brissopsis*** Agassiz, 1840

Diagnosis (modified from Mortensen, 1951; Kroh, 2005; Smith and Kroh, 2011)**:** Test ovate, somewhat depressed, with shallow frontal notch. Apical system with 4 genital pores. Ambulacrum III slightly depressed with differentiated pores, not crowded. Petals slightly to moderately sunken aborally, straight or flexed outwards in most species. Anterior petals no or slightly longer than posterior petals in most

species. Petal tips straight. Labrum broadly T-shaped, not extend beyond first ambulacral plate in most species. Sternal plates and episternal plates suture slightly close to posterior. Episternal plates trapezoidal, taper to posterior and indented by ambulacral plates. Plastron ultramphisternous or holamphisternous, with symmetric sternal and episternal plates.

Remarks: Most *Brissopsis*, as well as other spatangoids, are easily identifiable based on important morphological features such as general outlines, plating patterns, and fasciole forms. In the case of fossils, these characters may not be fully visible due to deformation and poor preservation. In our case, although it is easy to identify the genera *Brissopsis* and *Schizaster* for extant specimens, the fossil *Brissopsis* and *Schizaster* we found in the Gutingkeng Fm. shared a high similarity among each other. Due to strong deformation and preservation as internal molds, general outlines, plating patterns, and fasciole forms are not available on most specimens. The poor preservation of key diagnostic features makes identification challenging for the studied specimens. Especially, the lengths of certain features (e.g., widths of ambulacrum) can be affected by compression and deformation, causing specimens of several taxa to become very similar.

Fortunately, based on the preserved oral plating patterns, pore pairs in ambulacrum III, and clear aboral petal outlines on relatively well-preserved specimens, we can still identify members of the genera *Brissopsis* and *Schizaster* in some of the collected specimens. Members of *Brissopsis* exhibit differentiated pores in ambulacrum III, with both anterior and posterior petals flexed outwards and the length of anterior petals nearly equal to the posterior petals. In contrast, members of *Schizaster* display single series pore pairs in ambulacrum III, with both anterior and posterior petals flexed inwards and nearly tear-shaped, and the length of anterior petals significantly shorter than posterior petals.

The most obvious difference between these two taxa is their oral plating patterns. The plastron of *Schizaster* is mesamphisternous, characterized by an amphisternous plastron with near-symmetrical sternal plates and biserially offset episternal plates. In contrast, the plastron of *Brissopsis* is holamphisternous or ultramphisternous. The former features an amphisternous plastron with symmetrical sternal plates and symmetrical, undifferentiated episternal plates, while the latter displays an amphisternous plastron with symmetrical sternal plates followed by symmetrical but markedly different-sized and shaped episternal and other plates (Kroh, 2005).

Furthermore, the sternal plates of *Schizaster* are elongated, bringing the suture of them and following episternal plates very close to the posterior margin. Conversely, the sternal plates of *Brissopsis* are noticeably shorter than those of *Schizaster*, resulting in the suture being farther from the posterior margin. Additionally, the episternal plates of *Schizaste*r have a flattened hexagonal shape resembling a normal plate outline, whereas those of *Brissopsis* are trapezoidal, tapering towards the posterior due to indentation by widening ambulacral plates, followed by narrower second episternal plates also indented by widening ambulacral plates.

Brissopsis sp.

Figs. 5, 6(D), 8

Material: 16 specimens (ASIZF0100706, ASIZF0100707, ASIZF0100815 to ASIZF0100819, ASIZF0100827 to ASIZF0100833, ASIZF0100837, ASIZF0100839; Table S1, Appendix A).

Occurrence: Tianliao, Kaohsiung. Gutingkeng Fm., Lower Pleistocene.

Description: Test small to middle (mostly 4 to 6 cm in length), ovate to oval shaped (Figs. 5(A–C), 6(D)), slightly convex at posterior (Fig. 5(H)). Aboral surface flat without obvious slope (Fig. 5(H)), greatest height near posterior margin; narrow, slightly depressed ambulacrum III extending to oral surface at anterior (Figs. 5(A, B), 6(D)), with differentiated pores (Figs. 5(B), 6(D)). Apical system slightly near to posterior margin (Figs. 5(B), 6(D)), genital pores not obvious. Petals slightly depressed, rectangle shaped, nearly straight but slightly flexed outwards (Figs. 5(A, B), 6(D)). Anterior petals length similar to posterior petals (Figs. 5(B), 6(D)). Petal tips nearly straight (Figs. 5(A, B), 6(D)). Numbers of pore pairs about 15 to 20 in each ambulacrum (Figs. 5(B), 6(D)). Oral surface slightly convex (Fig. 5(G, H)). Peristome near anterior margin (Figs. 5(C–F), 8). Plastron slightly inflated, ovate, greatest width slightly close to posterior margin (Figs. 5(C), 8(B)). Periproct at posterior keel end, closer to greatest height (Fig. 5(G)). Peripetalous and lateroanal fasciole not obvious. Labrum short and wide, not extend beyond first ambulacral plate (Figs. 5(C–F), 8). Sternal plates slightly elongated, suture with episternal plates slightly near posterior margin (Figs. 5(C–F), 8). Episternal plates trapezoidal, taper to posterior and indented by ambulacral plates. Plastron holamphisternous, with symmetric sternal and episternal plates (Figs. 5(C–F), 8).

Remarks: The relatively short sunken petals, sunken ambulacrum III with differentiated pore pairs, a short and mushroom-shaped labrum, and trapezoidal episternal plates tapered to the posterior and indented by ambulacral plates suggest that they likely belong to the subfamily Brissopsinae (Mortensen, 1951; Kroh and Smith, 2010; Smith and Kroh, 2011). There are two genera under the subfamily Brissopsinae: *Brissalius* and *Brissopsis* (Kroh and Mooi, 2023). *Brissalius* is a monotypic genus with a member, *Brissalius vannoordenburgi*, primarily characterized by a distinct subanal fasciole pattern and posterior petals that are almost parallel, with an inner series of pore pairs reduced adapically. Due to the obviously different petal pattern, the studied specimens are unlikely to belong to genus *Brissalius*, and therefore belong to the genus *Brissopsis*.

Comparing the studied specimens to *Brissopsis luzonica*, the only extant *Brissopsis* species recorded in Taiwanese waters (Chen, pers. comm. 2023), the studied specimens obviously differ from it because they exhibit almost parallel posterior petals, implying that the studied specimens may not belong to any extant *Brissopsis* species found in Taiwanese waters, similar to the case of schizasteroid specimens.

5. Discussion

5.1. Spine preservation

While most of the studied specimens cannot be considered well-preserved fossils, a number of the fossil spatangoids were, in fact, found with their spines attached and thus show a remarkably preservation. In particular, the spines on ASIZF0100714 (Fig. S1; Appendix A) are abundant, with some even retaining their hollow structure. This specimen represents the first discovery of fossil spatangoids with spines attached among hundreds of reported fossil spatangoids in Taiwan.

Among the various adaptations facilitating their movement within fine-grained sediments, the morphological innovations and distribution of their spines play a particularly vital role (Walker and Gagnon, 2014). Melville and Durham (1966) provided an overview of the functions and arrangements of heart urchin spines (Table 1). In the studied specimen (ASIZF0100714), clusters of spines are well-preserved within the depressed ambulacra (Fig. S1; Appendix A). Based on their positions, these spines can be classified as type F spines of Melville and Durham (1966), which serve the function of forming protective arches over the petals.

5.2. Taphonomy

Hu and Tao (1986) proposed that some fossil mollusks, bryozoans and ostracods in the upper Gutingkeng Fm. were transported and subsequently buried at the depositional site. However, this interpretation may not be exactly correct in the studied irregular heart urchins, primarily due to the delicate nature of their tests. The thickness of the test in the studied spatagoid species is thinner than 0.3 mm. Furthermore, their random orientation and distribution within the bedrock, without other fossil fragments or skeletons in close contact (Fig. 2(B)), imply that no obvious reworking event occurred. Moreover, one specimen with preservation of intact spines (Fig. S1; Appendix A) may indicate these fossils were buried *in situ*, as spines are typically lost within four days after death (Nebelsick et al., 1997). However, in some cases, spatangoids can also be preserved in mass accumulations with spines attached (Nebelsick and Kroh, 2002). For example, *Echinocardium* accumulations with extensive spine-attached specimens from Middle Miocene deposits in Ukraine indicate that spines and thin test can still be well-preserved after transportation (Radwański and Wysocka, 2001). In a non-actively disturbed environment, the case of *Ova canalifera* from the northern Adriatic Sea also illustrates that its thin test can survive on the surface for an extended period (Nebelsick et al., 1997; Nebelsick, 2004), facilitating intense encrustation which may act as reinforcement of the skeleton (Nebelsick and Mancosu, 2021). Nevertheless, despite their fragile tests, spatangoids with thin skeletons can be preserved and contribute to the interpretation of paleoenvironments (see below).

5.3. Functional morphology

In general, test shape for spatangoid echinoids reflected their environmental adaptations (Kanazawa, 1992). For *Schizaster*, the wedged-shaped profile with aboral surface slope toward anterior margin of the studied specimens suggests an excellent ability to move within sediments by thrusting into the sediment in front and rocking its anterior end up and down (Smith, 1984; Kanazawa, 1992). Furthermore, their posteriorly located apical system, keeled interambulacrum V, long anterior petals, and short posterior petals represent an adaptation to deep burrowing (McNamara and Philip, 1980; Kroh and Nebelsick, 2003). However, comparing to schizasteroids interpreted as extremely deep burrowers such as *Schizaster*

eurynotus (Mancosu and Nebelsick, 2016) and *Ova* morphotype 2 (Mancosu and Nebelsick, 2019), the studied specimens exhibit significantly shallower and narrower anterior ambulacrum, shorter and straighter anterior petals, and shallower posterior petals. These features may suggest that the studied specimens are slightly shallower burrowers than those species. As for *Brissopsis*, the members of this taxon are interpreted as better adapted for shallow to moderately deep burrowing due to their slightly wedge-shaped test profile and the presence of well-developed fascioles (Mancosu and Nebelsick, 2016, 2017). Most extant members of the genus *Brissopsis* live in muddy to fine-grained sandy substrates, buried 1 to 10 cm below the sediment surface (Kanazawa, 1992; Mancosu and Nebelsick, 2017).

Nevertheless, the shape of tests may not be the only factor affecting burrowing depth. For example, sediment characteristics also play a crucial role (Mancosu and Nebelsick, 2016, 2019). Many species burrow at different depths depending on the nature of sediments (Saitoh and Kanazawa, 2012). Typically, muddy sediments and redox conditions imply shallow burrowing (Kroh and Nebelsick, 2003), as seen in the Gutingkeng Fm. This also suggests that spatangoids may have burrowed deeper in coarser-grained sediments, irrespective of their morphology.

In summary, combining the taphonomic conditions and the morphological advantages for slightly deep burrowing shown by both species, the paleoenvironmental scenario can be valuably reconstructed based on the observations of this potentially *in situ* assemblage.

5.4. Paleoenvironmental implications

For *Schizaster*, most extant species are typically found in neritic environments shallower than 100 m in depth (Mortensen, 1951). For instance, *Schizaster lacunosus* in Taiwan primarily inhabits inshore areas at depths ranging from 5 to 90 m (Chao, 2000). Moreover, *Schizaster* is recognized as a deep infaunal deposit-feeding echinoid, known for constructing funnels to the sediment surface and sanitary drains (Schinner, 1993). The presence of suitable soft substrates, particularly silts and fine-grained sands, plays the most significant role in determining the occurrence of *Schizaster* within their depth tolerance (Mancosu and Nebelsick, 2016, 2019). An excellent example is the abundant occurrence of *Ova canalifera* in the Gulf of Trieste, northern Adriatic Sea. This area represents a semi-enclosed shallow-water basin with a maximum depth of 25 m, demonstrating that the distribution of schizasterids is

primarily influenced by sedimentary facies and restricted in shallow water (Nebelsick et al., 1997).

In contrast, most extant species of *Brissopsis* occur in relatively deep oceans (Mortensen, 1951) and it is one of the deepest-dwelling echinoids (Néraudeau et al., 2001), although some species are also known to occur in shallow water (Mancosu and Nebelsick, 2017). For example, *Brissopsis lyrifera* occurs at depths between 5 and 2250 m (Mortensen, 1951; Mecho et al., 2014), with dense monospecific populations mostly found in deeper environments between 50 and 200 m (Féral et al., 1990; Hollertz et al., 1998).

In short, based on the comparison of the modern distribution of the taxa found in the assemblage, we can further infer the potential paleoenvironment. The dominance of both *Schizaster* and *Brissopsis* species implies that the paleoenvironment of this assemblage might have been suitable fine-grained soft substrates with low energy (Mortensen, 1951; Néraudeau et al., 2001; Kroh and Nebelsick, 2003), within a deeper shallow water setting but not exceeding the depth tolerance of *Schizaster* (upper sublittoral).

Interestingly, when compared to similar cases worldwide, the taxonomic composition of the spatangoid assemblage found in the Gutingkeng Fm. shares an extremely high similarity several assemblages. *Schizaster* and *Brissopsis* are the predominant echinoids occurring in many clays and mudstones in the basin deposits of the Early Miocene of the Central Paratethys (Kroh, 2003a, 2005). Another case is Assemblage 3 at the S'Archittu-Cajaragas section in the Miocene of Sardinia (Mancosu and Nebelsick, 2019). This low-diversity echinoid assemblage is dominated by *Brissopsis* and *Schizaster* (*Ova*) and found within a highly bioturbated, whitish mud- to wackestone. Based on detailed taphonomic and sedimentological features and functional morphological examination, this fauna is interpreted as inhabiting a deeper, soft-bottom environment, possibly below storm-wave base. The results of the investigations presented here also show that echinoids can be used as excellent paleoenvironmental indicators and can be closely compared to faunas from other geographic areas.

5.5. Distribution of Schizaster*-rich echinoid assemblages in Taiwan*

The *Schizaster*-rich echinoid assemblages are among the best echinoid records in Taiwan. The earliest records occur in the Slate Belt in NE Taiwan. Tokunaga

(1903) reported an indeterminate species of *Schizaster* from the Oligocene Tatungshan Fm. in Yilan, northern Taiwan. Subsequently, Nisiyama (1933) presented a preliminary report on a new species of *Schizaster* (*Paraster*) in Taiwan. Hayasaka (1948b) further identified *Schizaster taiwanicus* Hayasaka, 1948 and an indeterminable *Schizaster* species within the Tatungshan and Kankou formations in northern Taiwan.

The presence of *Schizaster* fossils within sedimentary strata had received limited attention until the work of Cheng and Wang (1981). Their ground-breaking work documented a *Schizaster* echinoid assemblage form the Middle Miocene lower Nangang Fm. (also known as the Tsouho Fm.) in northern Taiwan. These fossils were identified as belonging to *Schizaster taiwanicus* and an as-yet-undescribed species. More recently, amateur collectors have reported new occurrences of *Schizaster lacunosus* in the Lower Pleistocene Liuchungchi Fm. (Huang, 2011) and *Schizaster* (*Ova*) sp. in the Lower Miocene Taliao Fm. (Chiang, pers. comm. 2023). Additionally, Chuang (2020) reported the presence of a *Schizaster* (*Ova*) sp. in the Lower Pleistocene Yujing Shale in southern Taiwan.

Interestingly, the distribution of *Schizaster*-rich echinoid assemblages in Taiwan exhibits distinct temporal and geographical patterns, which can be categorized into two notable groups (Fig. 9; Table 2). For deposits older than the Pliocene, *Schizaster* fossils have been extensively documented in northern Taiwan, including the Oligocene Slate Belt, the Lower Miocene Taliao Fm., and the Middle Miocene Nangang Fm. However, for deposits younger than the Pliocene, *Schizaster* fossils became scarce in northern Taiwan, while they still thrived in the southern region. This divergence in distribution can potentially be linked to paleoenvironmental changes resulting from the most recent orogenic events, estimated to have occurred around 6.5 Ma (Lin et al., 2003). Prior to the orogeny, Taiwan was located at a stable passive continental margin (Lin et al., 2003). In the deeper continental shelf, situated far from the sediment sources, muddy protoliths of the Slate Belt formed, providing a habitat for abundant *Schizaster*-rich echinoid assemblages. Closer to the southeastern coast of China along the continental shelf, several *Schizaster* communities coexisted with other spatangoids (Wang, 1984a; Huang, 2011).

Following the orogeny, foreland basins began to develop in what is now the Taiwan Strait. These basins accumulated extensive sediments from the rising island of Taiwan (Lin et al., 2003). The rapid infilling of these basins by immature sediment

led to a swift shallowing of the sedimentary environment and coarsening of substrate (Lin et al., 2003), resulting in the local disappearance of *Schizaster*-rich echinoid assemblages in the strata of northern Taiwan. During this period, due to the persistence of relatively finer substrate and deeper environments (Nagel et al., 2013), southern Taiwan emerged as a local refuge for *Schizaster*. These conditions facilitated the continued presence of dense *Schizaster* communities in southern Taiwan, as discovered in our study. This shift in distribution and abundance seen in irregular echinoids can potentially be attributed to the significant paleoenvironmental changes that followed the orogeny and the subsequent alteration of sedimentary conditions in the region.

5.6. Fossil distortion implication

Estimating strain in rocks plays a pivotal role in studying deformation within orogenic belts. Structural geologists commonly select objects with identifiable original shape to serve as strain markers in rocks (Ramsay, 1967; Ramsay and Huber, 1983). Among the various strain markers, bilaterally symmetric invertebrate fossils are frequently chosen due to their widespread occurrence and their suitability for retrodeformation (e.g., Wellman method; Wellman, 1962). Recently, irregular echinoid fossils, which also exhibit bilateral symmetry, have been introduced as strain markers within Quaternary strata in Taiwan (Tseng, 2023).

It is important to note that not all fossils are equally reliable as strain markers, particularly those lacking thick and robust hard skeletons. The sediment load during compaction can result in the compression of these “fragile fossils”. Consequently, these fossils may preserve more diagenesis-related information rather than serving as accurate indicators of deformation during orogeny.

A notable example of this phenomenon can be seen in the case of fossil spatangoids. Our observations have revealed that due to their extremely thin tests and fragility, spatangoid specimens exhibit significant deformation, even in the absence of metamorphism (Fig. 10). Furthermore, among the studied specimens preserved with the bedrocks (n = 5), all exhibit distinct flattened deformation parallel to the bedding plane, accompanied by radial cracks along plate boundary at the edges (Fig. 5(C)). These observations support the inference that the deformation is attributable to sediment load rather than tectonic stresses, which predominantly dictate the variation in deformation direction and type under different stress

conditions (Boyd and Motani, 2008). This finding suggests that the abundant fossil spatangoids found in low-grade metamorphic rocks, such as the Taiwan's Slate Belt, where the protolith is mudstone, might not be suitable as reliable strain markers for recording tectonic events.

In summary, the robustness of an echinoid fossil may be a pivotal factor influencing its viability as a dependable strain marker. In contrast to our study, Tseng (2023) effectively employed the fossil sand dollar *Scaphechinus mirabilis* as a strain marker to derive regional tectonic implications in the Miaoli area of central Taiwan; the success may be attributed to the robust test of *Scaphechinus*, which boasts a thickness at least five times greater than that of the spatangoids studied here. On the other hand, unlike heart urchins, *S. mirabilis* possesses buttress support and internal pillars that contribute to strengthening the test architecture (Lin et al., 2021b), which could also be a significant factor. Our findings underscore that using echinoids for deformation implications should be very careful due to the variability in test robustness and the special disarticulation influenced by multiple plating.

Data availability

Data used for this paper are specimens held in museum collections.

Declaration of Competing Interest

The authors declare that they have no known competing financial interests or personal relationships that could have appeared to influence the work reported in this paper.

Acknowledgments

This work was supported by the National Science and Technology Council, Taiwan (Grant No. 112-2116-M-001-017-MY3) and Academia Sinica, Taipei, Taiwan to C.-H. Lin. We thank Chia-Ching Chen and Cheng-Kai Chiang for providing the samples used in this study. We thank Kun-Hsuan Lee and Kai-Jun Zhang for their discussion related to this research. We thank Leighton Lin, Shao-En Yen, Wei-Heng Lee, Yun-Ting Lin, Ting-En Wang, Tomáš Přikryl, Meng-Chen Ko, Li-You Lin, Li-Li Lin, Li-Man Lin, Junko Kurosaki, and the members of Marine Paleontology Lab, BRCAS (https://otolithlin.biodiv.tw) for their assistance in the field. We thank Gilles Escarguel, Bertrand Lefebvre, Didier Néraudeau, James Nebelsick, Andreas Kroh,

and one anonymous reviewer for their valuable comments and suggestions on earlier versions of this article.

Appendix A. Supplementary information

Supplementary information (including Table S1 and Fig. S1) associated with this article can be found, in the online version, at:

References

Boivin, S., Saucède, T., Laffont, R., Steimetz, E., Neige, P., 2018. Diversification rates indicate an early role of adaptive radiations at the origin of modern echinoid fauna. PLoS One 13, e0194575.

Boyd, A.A., Motani, R., 2008. Three-dimensional reevaluation of the deformation removal technique based on “jigsaw puzzling”. Palaeontologia Electronica 11, 2.

Chao, S.M., 2000. The irregular sea urchin (Echinodermata: Echinoidea) from Taiwan, with descriptions of six new records. Zoological Studies 39, 250–265.

Chen, H.K., Hsu, C.H., Lin, J.P., in press. Three echinoid assemblages with the earliest cidaroid (Echinodermata: Echinoidea) fossil record from the Middle Miocene of Taiwan. Geobios, https://doi.org/10.1016/j.geobios.2024.05.010.

Chen, W.S., 2016. An introduction to the geology in Taiwan. Geological Society of Taiwan, Taipei, 204 p. (in Mandarin).

Cheng, Y.M., Wang, C.C., 1981. Preliminary report on the fossil echinoids from the Miocene Tsouho Formation of Hsintien, northern Taiwan. Ti-Chih 3, 151–155 (in Mandarin).

Chuang, S.C., 2020, Study of the echinoid fossils from Yujing Area, Tainan. M.Sc. thesis, National Cheng Kung University, Tainan, Taiwan (unpubl.).

Féral, J.P., Ferrand, J.G., Guille, A., 1990. Macrobenthic physiological responses to environmental fluctuations: the reproductive cycle and enzymatic polymorphism of a eurybathic sea-urchin on the Northwestern Mediterranean continental shelf and slope. Continental Shelf Research 10, 1147–1155.

Filander, Z., Griffiths, C., 2017. Illustrated guide to the echinoid (Echinodermata: Echinoidea) fauna of South Africa. Zootaxa 4296, 1–72.

Hayasaka, I., 1948a. Notes on some fossil echinoids of Taiwan, III. Acta Geologica Taiwanica 1, 111–128.

Hayasaka, I., 1948b. Notes on some fossil echinoids of Taiwan, IV. Acta Geologica Taiwanica 2, 85–124.

Hayasaka, I., Morishita, A., 1947a. Notes on some fossil echinoids of Taiwan, II. Acta Geologica Taiwanica 1, 93–110.

Hayasaka, I., Morishita, A., 1947b. Fossil species of *Clypeaster* from Taiwan. Acta Geologica Taiwanica 1, 39–57.

Ho, S.L., Wang, J.K., Lin, Y.J., Lin, C.R., Lee, C.W., Hsu, C.H., Chang, L.Y., Wu, T.H., Tseng, C.C., Wu, H.J., John, C.M., Oji, T., Liu, T.K., Chen, W.S., Li, P., Fang, J.N., Lin, J.P., 2022. Changing surface ocean circulation caused the local demise of echinoid *Scaphechinus mirabilis* in Taiwan during the Pleistocene–Holocene transition. Scientific Reports 12, 8204.

Hollertz, K., Skold, M., Rosenberg, R., 1998. Interactions between two deposit feeding echinoderms: the spatangoid *Brissopsis lyrifera* (Forbes) and the ophiuroid *Amphiura chiajei* (Forbes). Hydrobiologia 376, 287–295.

Hopkins, M.J., Smith, A.B., 2015. Dynamic evolutionary change in post-Paleozoic echinoids and the importance of scale when interpreting changes in rates of evolution. Proceedings of the National Academy of Sciences, USA 112, 3758–3763.

Horng, C.S., Shea, K.S., 1994. Study of nannofossil biostratigraphy in the eastern part of the Erhjen-Chi section, southwestern Taiwan. Special Publication of the Central Geological Survey 8, 181–204.

Hu, C.H., 1987. Bryozoan faunas from the Kutingkeng Formation (Pliocene), Fengshan Reservoir, southern Taiwan. Annual of Taiwan Museum 40, 15–50.

Hu, C.H., Tao, S.J., 1982. A new species of solitary corals and associated fossils from the lower Gutingkeng Formation of Taiwan. Ti-Chih 4, 39–46 (in Mandarin).

Hu, C.H., Tao, S.J., 1986. Fossil ostracods from the Fengshan water reservoir, Kaohsiung district, southern Taiwan. Acta Geologica Taiwanica 24, 51–65.

Hu, C.H., Tao, S.J., 1992. Taiwan shellfish fossil record. National Museum of Natural Science, Taichung 2, 571–647 (in Mandarin).

Huang, C.C., 2011. Taiwanese echinoids I. Private press, Taichung, 208 p. (in Mandarin).

Huang, C.C., 2015. Taiwanese echinoids II. Private press, Taichung, 124 p. (in Mandarin).

Kanazawa, K., 1992. Adaptation of test shape for burrowing and locomotion in spatangoid echinoids. Palaeontology 35, 733–750.

Kroh, A., 2003a. Echinoderms of the Karpatian. In: Brzobohatý, R., Cicha, I., Kováč, M., Rögl, F. (Eds.), The Karpatian: A Lower Miocene Stage of the Central Paratethys, pp. 247–256.

Kroh, A., 2003b. Palaeobiology and biogeography of a Danian echinoid fauna of Lower Austria. In: Féral, J.P., David, B. (Eds.), Echinoderm Research 2001: Proceedings of the Sixth European Conference on Echinoderm Research, Banyuls-sur-mer, France, 3–7 September 2001, pp. 69–75.

Kroh, A., 2005. Band 2. Echinoidea neogenica. In: Piller, W.E. (Ed.), Catalogus Fossilium Austriae. Österreichische Akademie der Wissenschaften, Wien, 210 p.

Kroh, A., Mooi, R., 2023. World Echinoidea Database. https://www.marinespecies.org/echinoidea (accessed 9/17/2023).

Kroh, A., Nebelsick, J.H., 2003. Echinoid assemblages as a tool for palaeoenvironmental reconstruction – an example from the Early Miocene of Egypt. Palaeogeography, Palaeoclimatology, Palaeoecology 201, 157–177.

Kroh, A., Smith, A.B., 2010. The phylogeny and classification of post-Palaeozoic echinoids. Journal of Systematic Paleontology 8, 147–212.

Kuo, C.Y., 2023. Study of fossil echinoderms from Erliao, Zuojhen, Tainan, Taiwan. M.Sc. thesis, National Taiwan Normal University, Tainan, Taiwan (unpubl.).

Lee, H., Lee, K.S., Hsu, C.H., Lee, C.W., Li, C.E., Wang, J.K., Tseng, C.C., Chen, W.J., Horng, C.C., Ford, C.T., Kroh, A., Bronstein, O., Tanaka, H., Oji, T., Lin, J.P., Janies, D., 2023. Phylogeny, ancestral ranges and reclassification of sand dollars. Scientific Reports 13, 10199.

Lewis, D.N., Donovan, S., 2007. A standardized method of describing fossils, using Echinoidea as an example. Scripta Geologica 134, 109–118.

Lin, A.T., Watts, A.B., Hesselbo, S.P., 2003. Cenozoic stratigraphy and subsidence history of the South China Sea margin in the Taiwan region. Basin Research 15, 453–478.

Lin, C.H., Wu, S.M., Lin, C.Y., Chien, C.W., 2023. Early Pliocene otolith assemblages from the outer-shelf environment reveal the establishment of mesopelagic fish fauna over 3 million years ago in southwestern Taiwan. Swiss Journal of Palaeontology 142, 23.

Lin, C.W., 2013. Geological map of Taiwan, Qishan, scale 1:50,000. Taiwan Central Geological Survey, Taipei.

Lin, C.H., Chien, C.W., Lee, S.W., Chang, C.W., 2021a. Fish fossils of Taiwan: a review and prospection. Historical Biology 33, 1362–1372.

Lin, Y.J., Fang, J.N., Chang, C.C., Cheng, C.C., Lin, J.P., 2021b. Stereomic microstructure of Clypeasteroida in thin section based on new material from Pleistocene strata in Taiwan. Terrestrial, Atmospheric and Oceanic Sciences 32, 1093–1105.

Mancosu, A., Nebelsick, J.H., 2016. Echinoid assemblages from the early Miocene of Funtanazza (Sardinia): A tool for reconstructing depositional environments along a shelf gradient. Palaeogeography, Palaeoclimatology, Palaeoecology 454, 139–160.

Mancosu, A., Nebelsick, J.H., 2017. Palaeoecology and taphonomy of spatangoid-dominated echinoid assemblages: A case study from the Early-Middle Miocene of Sardinia, Italy. Palaeogeography, Palaeoclimatology, Palaeoecology 466, 334–352.

Mancosu, A., Nebelsick, J.H., 2019. Paleoecology of sublittoral Miocene echinoids from Sardinia: A case study for substrate controls of faunal distributions. Journal of Paleontology 93, 764–784.

McNamara, K.J., 1995. The spatangoid echinoid *Schizaster* (*Schizaster*) *compactus* (Koehler, 1914) in Western Australia. Records of the Western Australian Museum 17, 315–323.

McNamara, K.J., Philip, G.M., 1980. Tertiary species of *Echinolampas* (Echinoidea) from southern Australia. Memoirs of the National Museum of Victoria 41, 1–14.

Mecho, A., Billett, D.S.M., Ramírez-Llodra, E., Aguzzi, J., Tyler, P.A., Company, J.B., 2014. First records, rediscovery and compilation of deep-sea echinoderms in the middle and lower continental slope of the Mediterranean Sea. Scientia Marina 78, 281–302.

Melville, R.V, Durham, J.W., 1966. Skeletal morphology. In: Moore, R.C. (Ed.), Treatise on Invertebrate Palaeontology Part U. Echinodermata 3 (Asterozoans, Echinozoans). The Geological Society of America, Inc. and the University of Kansas Press, Boulder and Lawrence, U220–U257.

Mondiardino Koch, N., Thompson, J.R., 2020. A total-evidence dated phylogeny of Echinoidea combining phylogenomic and paleontological data. Systematic Biology 70, 421–439.

Mortensen, T., 1951. A Monograph of the Echinoidea. V, 2. Spatangoida II. Amphisternata II. Spatangidae, Loveniidae, Pericosmidae, Schizasteridae, Brissidae. Carl Andreas Reitzel, Copenhagen, 593 p.

Nagel, S., Castelltort, S., Wetzel, A., Willett, S.D., Mouthereau, F., Lin, A.T., 2013. Sedimentology and foreland basin paleogeography during Taiwan arc continent collision. Journal of Asian Earth Sciences 62, 180–204.

Nebelsick, J.H., 2004. Taphonomy of Echinoderms: introduction and outlook. In: Heinzeller, T., Nebelsick, J.H. (Eds.), Echinoderms München. Proceedings of the 11th International Echinoderm Meeting. Taylor & Francis, Rotterdam, pp. 471–478.

Nebelsick, J.H., Kroh, A., 2002. The stormy path from life to death assemblages: the formation and preservation of mass accumulations of fossil sand dollars. Palaios 17, 378–393.

Nebelsick, J.H., Mancosu, A., 2021. The taphonomy of echinoids: skeletal morphologies, environmental factors, and preservation pathways (Elements of Paleontology). Cambridge University Press, Cambridge, 52 p.

Nebelsick, J.H., Schmid, B., Stachowitsch, M., 1997. The encrustation of fossil and recent sea-urchin tests: ecological and taphonomic significance. Lethaia 30, 271–284.

Néraudeau, D., Goubert, E., Lacour, D., Rouchy, J.M., 2001. Changing biodiversity of Mediterranean irregular echinoids from the Messinian to the Present-Day. Palaeogeography, Palaeoclimatology, Palaeoecology 175, 43–60.

Nisiyama, S., 1933. Echinoidea. In: Koza, I. (Ed.), Iwanami's manual of geology and paleontology. Iwanami Shoten, Tokyo 3, 1–60.

Nisiyama, S., 1968. The echinoid fauna from Japan and adjacent regions II. Special Papers Paleontological Society of Japan 13, 1–491.

Pereira, B.C., 2015. Echinoid diversity through time. In: Zamora, S., Rábano, I. (Eds.), Progress in echinoderm paleobiology. Cuadernos del Museo Geominero 19, pp. 133–136.

Radwański, A., Wysocka, A., 2001. Mass aggregation of Middle Miocene spine-coated echinoids *Echinocardium* and their integrated eco-taphonomy. Acta Geologica Polonica 51, 295–316.

Ramsay, J.G., 1967. Folding and fracturing of rocks. McGraw Hill, New York, 568 p.

Ramsay, J.G., Huber, M.I., 1983. The techniques of modern structural geology, volume 1: Strain analysis. Academic Press Incorporation, London, pp. 308–700.

Saitoh, M., Kanazawa, K., 2012. Adaptative morphology for living in shallow water environments in spatangoid echinoids. Zoosymposia 7, 255–265.

Schinner, G.O., 1993. Burrowing behavior, substrate preference, and distribution of *Schizaster canaliferus* (Echinoidea: Spatangoida) in the northern Adriatic Sea. Marine Ecology 14, 129–145.

Schultz, H., 2009. Sea urchins II, worldwide irregular deep water species. Heinke & Peter Schultz Partner Scientific Publications, Hemdingen, 349 p.

Shea, K.S., Horng, C.S., 1999. Recognition of the Pliocene-Pleistocene boundary based on *Pulleniatina* coiling change: A case study of the Erhjen-chi section, southwestern Taiwan. Quaternary Sciences 6, 549–555 (in Mandarin).

Smith, A.B., 1984. Echinoid palaeobiology. Allen and Unwin, London, 190 p.

Smith, A.B., Kroh, A., 2011. The Echinoid Directory. http://www.nhm.ac.uk/research-curation/projects/echinoid-directory (accessed 9/17/2023).

Sprinkle, J., 1980. An overview of the fossil record. In: Broadhead, T.W., Waters, J.A. (Eds.), Echinoderms, Notes for a short course. University of Tennessee Department of Geological Sciences, Studies in Geology 3, pp. 15–26.

Tokunaga, S., 1903. On the fossil echinoids of Japan. The Journal of the College of Science, Imperial University of Tokyo, Japan 17, 1–27.

Tseng, C.C., 2023, Fossil earthquakes preserves on fossils: A case study of deformed specimens of *Scaphechinus mirabilis* from Miaoli, Taiwan. M.Sc. thesis, National Taiwan University, Taipei, Taiwan (unpubl.).

Walker, D.E., Gagnon, J.M., 2014. Locomotion and functional spine morphology of the heart urchin *Brisaster fragilis*, with comparisons to *B. latifrons*. Journal of Marine Sciences 2014, 297631.

Wang, C.C., 1984a. A new species of *Pericosmus* (Echinoidea) from the Miocene Nankang Sandstone of northern Taiwan. Special Publication of the Central Geological Survey 3, 249–256.

Wang, C.C., 1984b. New classification of clypeasteroid echinoids. Proceedings of the Geological Society of China 27, 119–152.

Wang, C.C., 1985. Fossil clypeasterid echinoids from Taiwan. Proceedings of the Geological Society of China 28, 143–176.

Wang, C.C., 1986. Fossil astriclypeid echinoids from Taiwan. Proceedings of the Geological Society of China 29, 149–183.

Wang, Q.M., 1992. Paleoecology of the Pleistocene benthic foraminifers of the Chishan section, southwestern Taiwan. M.Sc. thesis, National Taiwan University, Taipei, Taiwan (unpubl.).

Wellman, H.G., 1962. A graphic method for analyzing fossil distortion caused by tectonic deformation. Geological Magazine 99, 348–352.

Table and Figure captions

Table 1. Spine classification of heart urchins (modified from Melville and Durham, 1966).

Table 2. List of the occurrences of fossil and extant *Schizaster* and *Brissopsis* in Taiwan.

Fig. 1. Geological and geographical background of the sampling site. **A.** Overview. **B.** Map showing the location of the sampling site (modified from Google Earth). **C.** Stratigraphic column (modified from Horng and Shea, 1994; Shea and Horng, 1999; Chen, 2016). **D.** Geological map of the sampling site (modified from Lin, 2013). Red star: sampling site.

Fig. 2. Photographs from the field. **A.** Overview of the sampling site. **B.** Surface-exposed spatangoid fossil. Red arrow: spatangoid fossil in B.

Fig. 3. Structure, anatomy and oral plating of spatangoid. Extant *Schizaster lacunosus* (ASIZE0000061) is used as an example.

Fig. 4. *Schizaster* sp. from the Gutingkeng Formation, Tianliao, Kaohsiung, Taiwan. **A.** Aboral view of ASIZF0100704. **B.** Aboral view of ASIZF0100810. **C.** Aboral view of ASIZF0100813. **D.** Posterior view of ASIZF0100704. **E.** Aboral view of ASIZF0100811. **F.** Left lateral view of ASIZF0100704. **G.** Oral view of ASIZF0100814. **H.** Oral view of ASIZF0100812. **I.** Oral view of ASIZF0100813. Scale bar: 20 mm.

Fig. 5. *Brissopsis* sp. from the Gutingkeng Formation, Tianliao, Kaohsiung, Taiwan. **A.** Aboral view of ASIZF0100815. **B.** Aboral view of ASIZF0100816. **C.** Oral view of ASIZF0100818. **D.** Oral view of ASIZF0100815. **E.** Oral view of ASIZF0100816. **F.** Oral view of ASIZF0100819. **G.** Posterior view of ASIZF0100815. **H.** Left lateral view of ASIZF0100816. Scale bar: 20 mm.

Fig. 6. Aboral outlines and the preserved pore pairs of *Schizaster* sp. and *Brissopsis* sp. **A-C.** *Schizaster* sp. A: ASIZF0100810; B: ASIZF0100704; C: ASIZF0100811. **D.** *Brissopsis* sp., ASIZF0100816. Oral area shaded. Scale bar: 10 mm.

Fig. 7. Oral plating of *Schizaster* sp. **A.** ASIZF0100812. **B.** ASIZF0100814. Interambulacra shaded in bright gray. Oral area shaded in deep gray. Scale bar: 10 mm.

Fig. 8. Oral plating of *Brissopsis* sp. **A.** ASIZF0100816. **B.** ASIZF0100818. **C.** ASIZF0100815. **D.** ASIZF0100819. Interambulacra shaded. Scale bar: 20 mm.

Fig. 9. Geographic and stratigraphic distributions of fossil *Schizaster* in Taiwan. The corresponding lithology are indicated. Stratigraphic columns and general interpretations on the sedimentary conditions are modified from Chen (2016). Geographic distribution of fossil *Schizaster* with colors indicating the geological ages of the localities (data from Hayasaka, 1948b; Cheng and Wang, 1981; Huang, 2011, 2015; Chuang, 2020; this study). All occurrences are listed in Table 2.

Fig. 10. Comparison of spatangoid fossils from sedimentary rocks (**A, B**) and low-grade metamorphic rocks (**C, D**) in Taiwan. A, B: Spatangoid sp. indet. (ASIZF0100713) from mudstone, Gutingkeng Formation, Early Pleistocene, in aboral (A) and left lateral (B) views; C, D: *Schizaster* sp. (ASIZF0100702) from argillite, Kankou Formation (Slate Belt), Oligocene, in aboral (C) and left lateral (D) views. Scale bars: 10 mm.

Figure 1

Click here to access/download;Figure;Figure 1 OK.tif

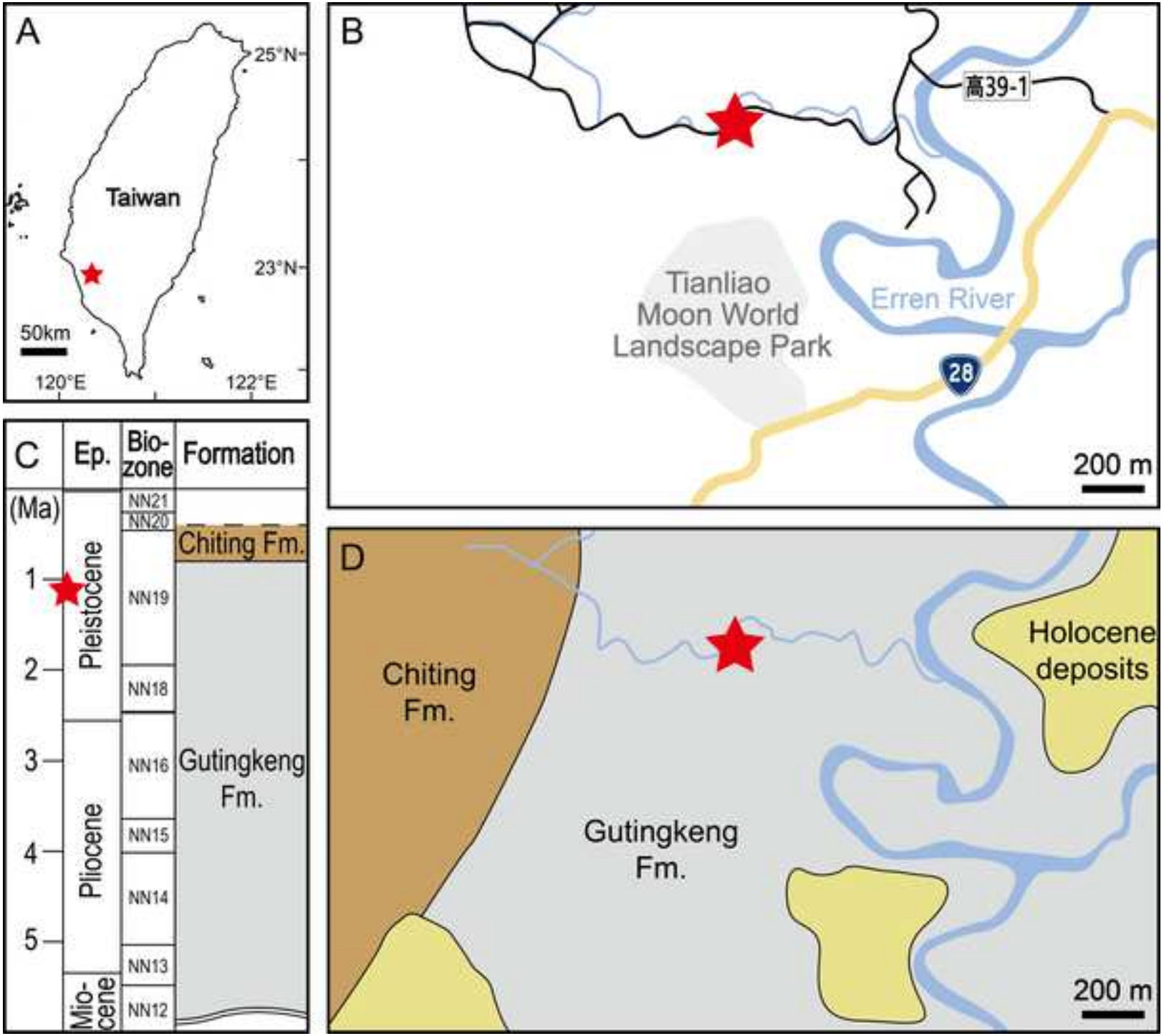

Figure 2

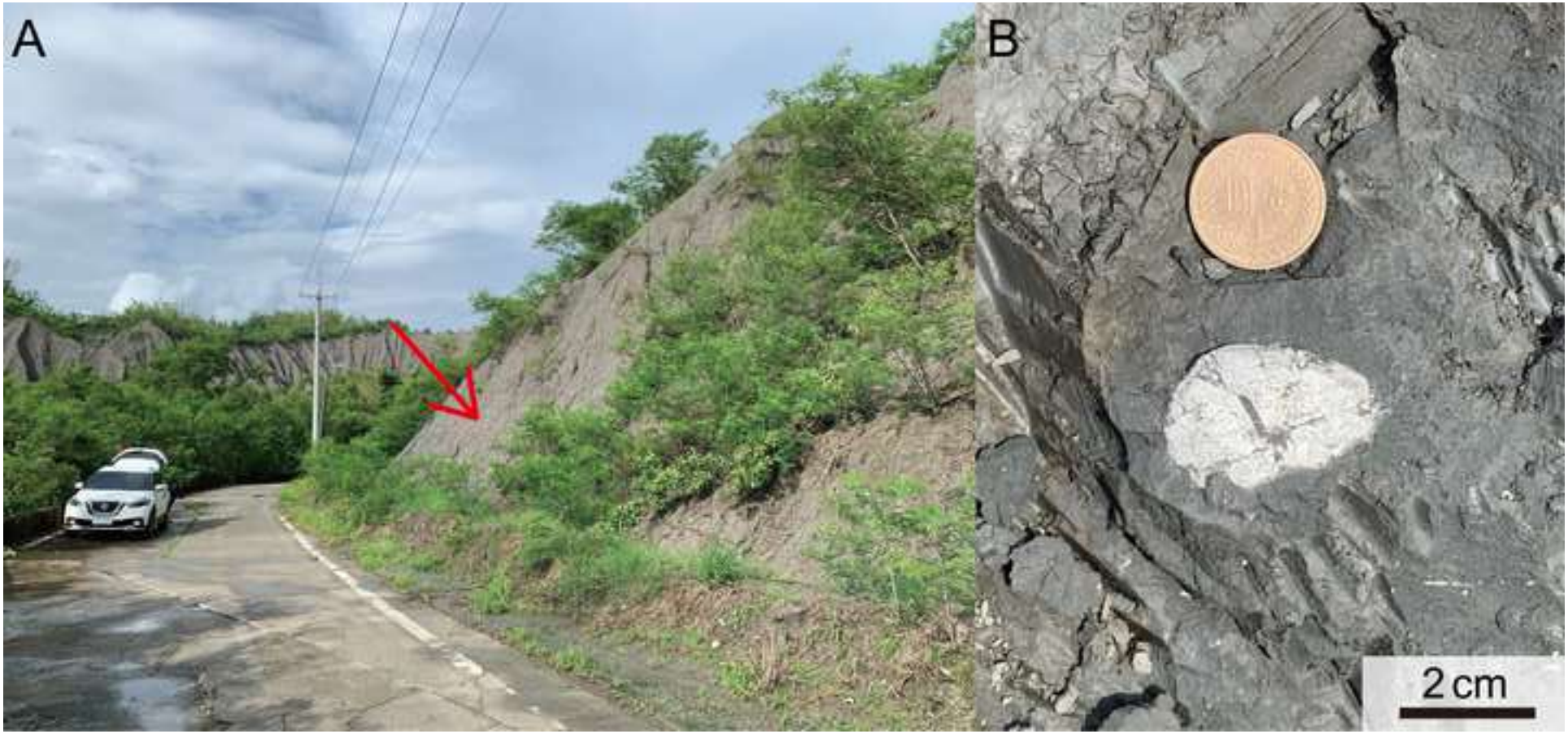

Figure 3

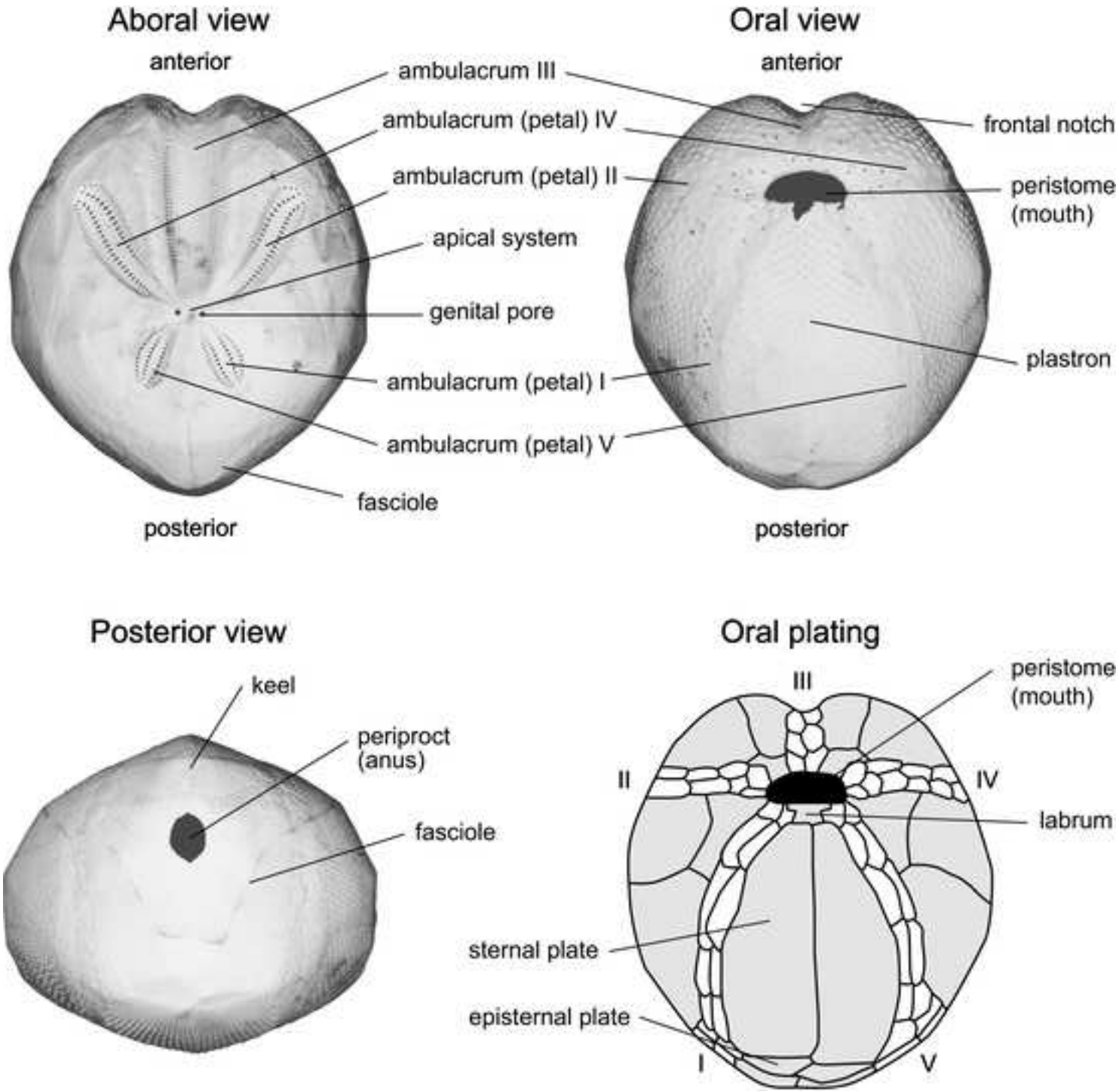

Figure 4

Click here to access/download;Figure;Figure 4 OK.tif

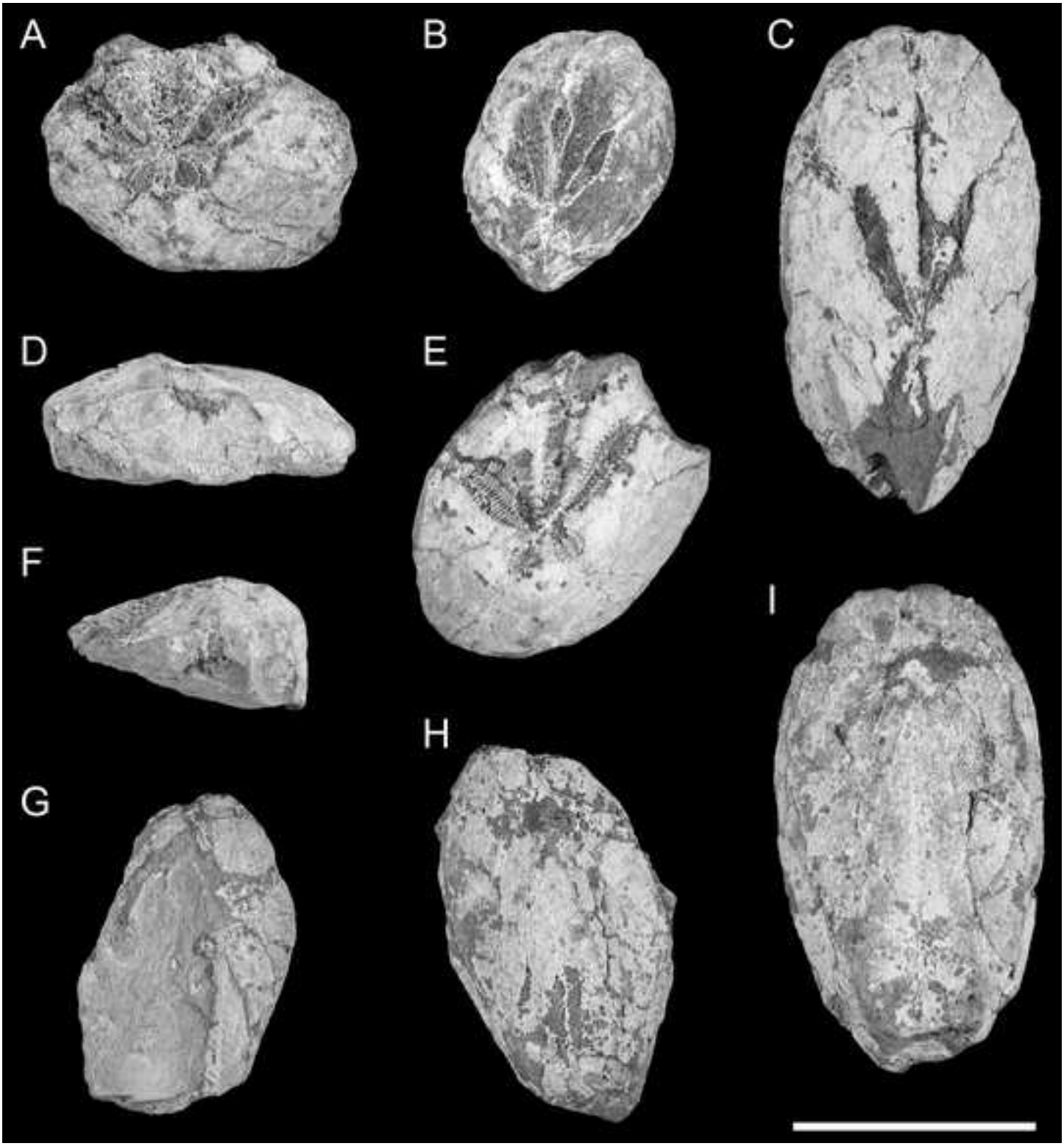

Figure 5

Click here to access/download;Figure;Figure 5 OK.tif

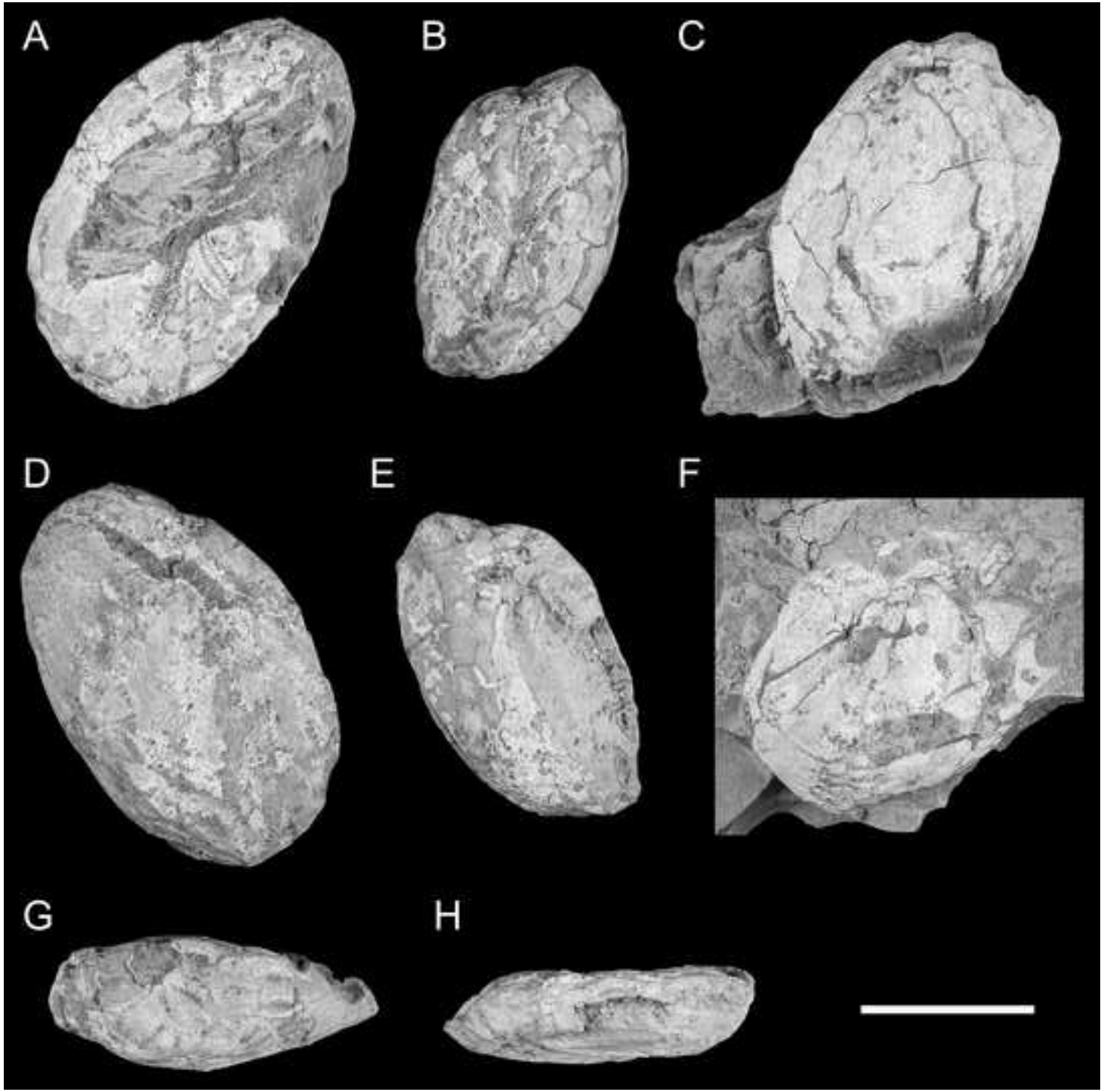

Figure 6

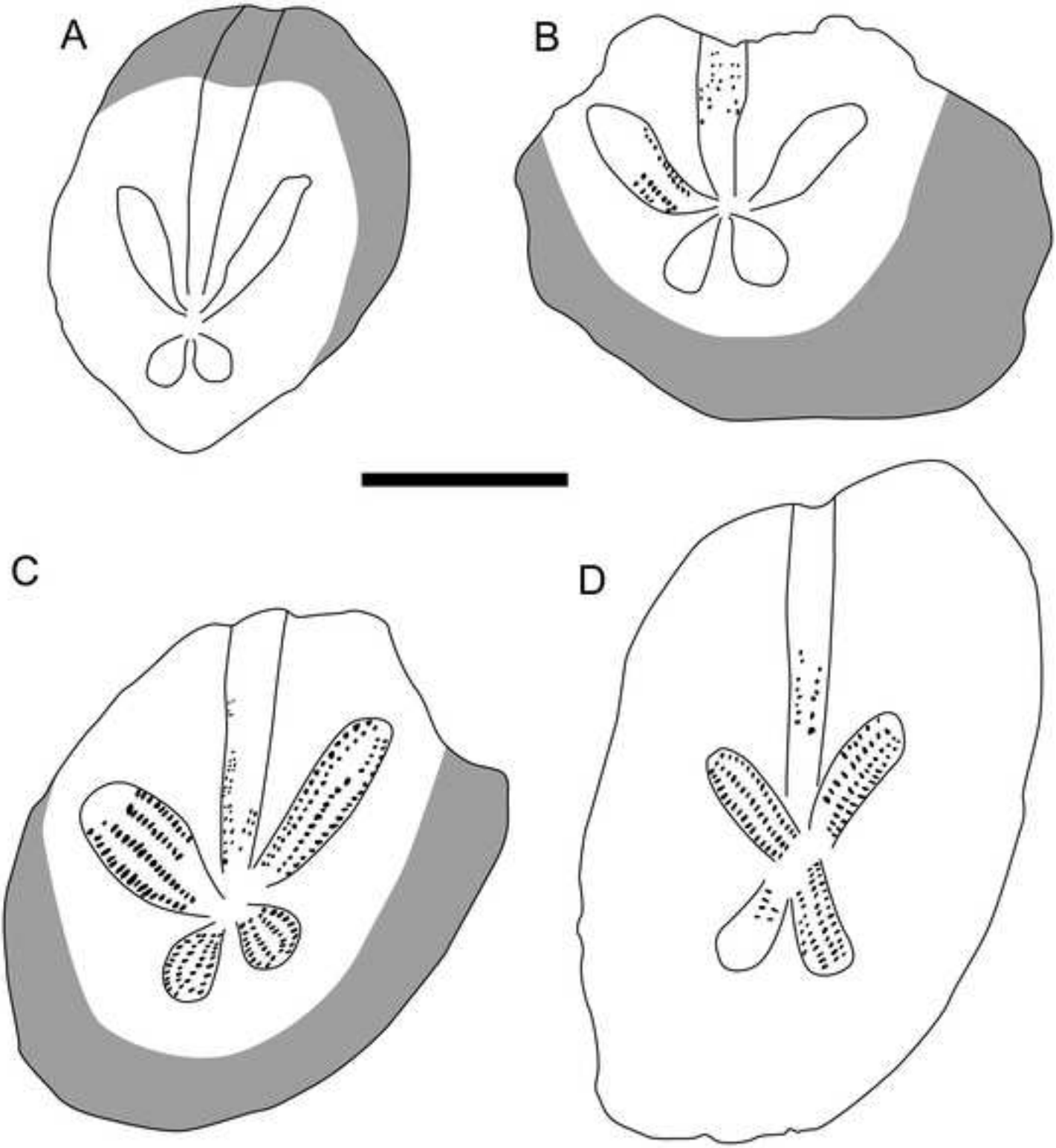

Figure 7

Click here to access/download;Figure;Figure 7 OK.tif

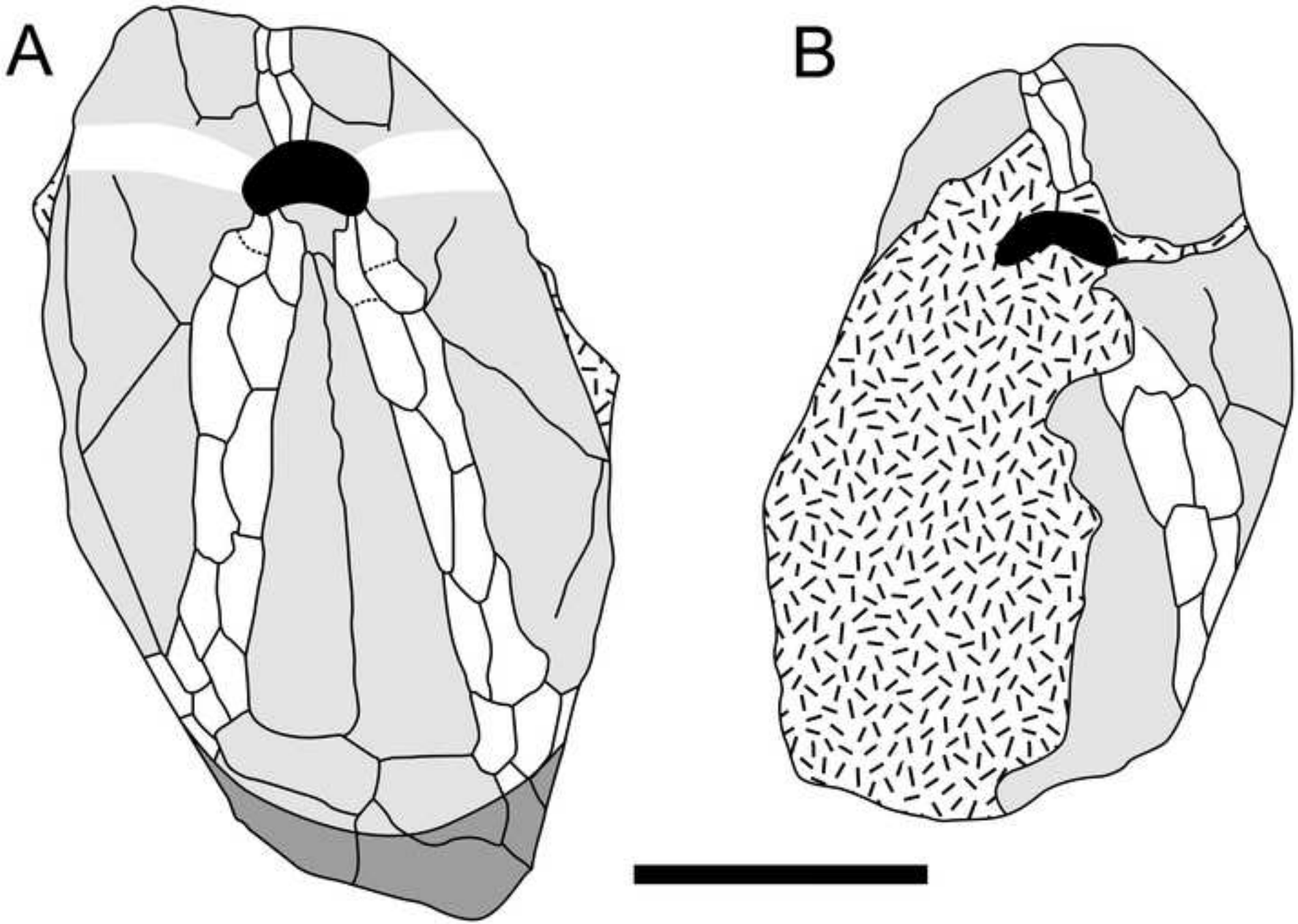

Figure 8

Click here to access/download;Figure;Figure 8 OK.tif

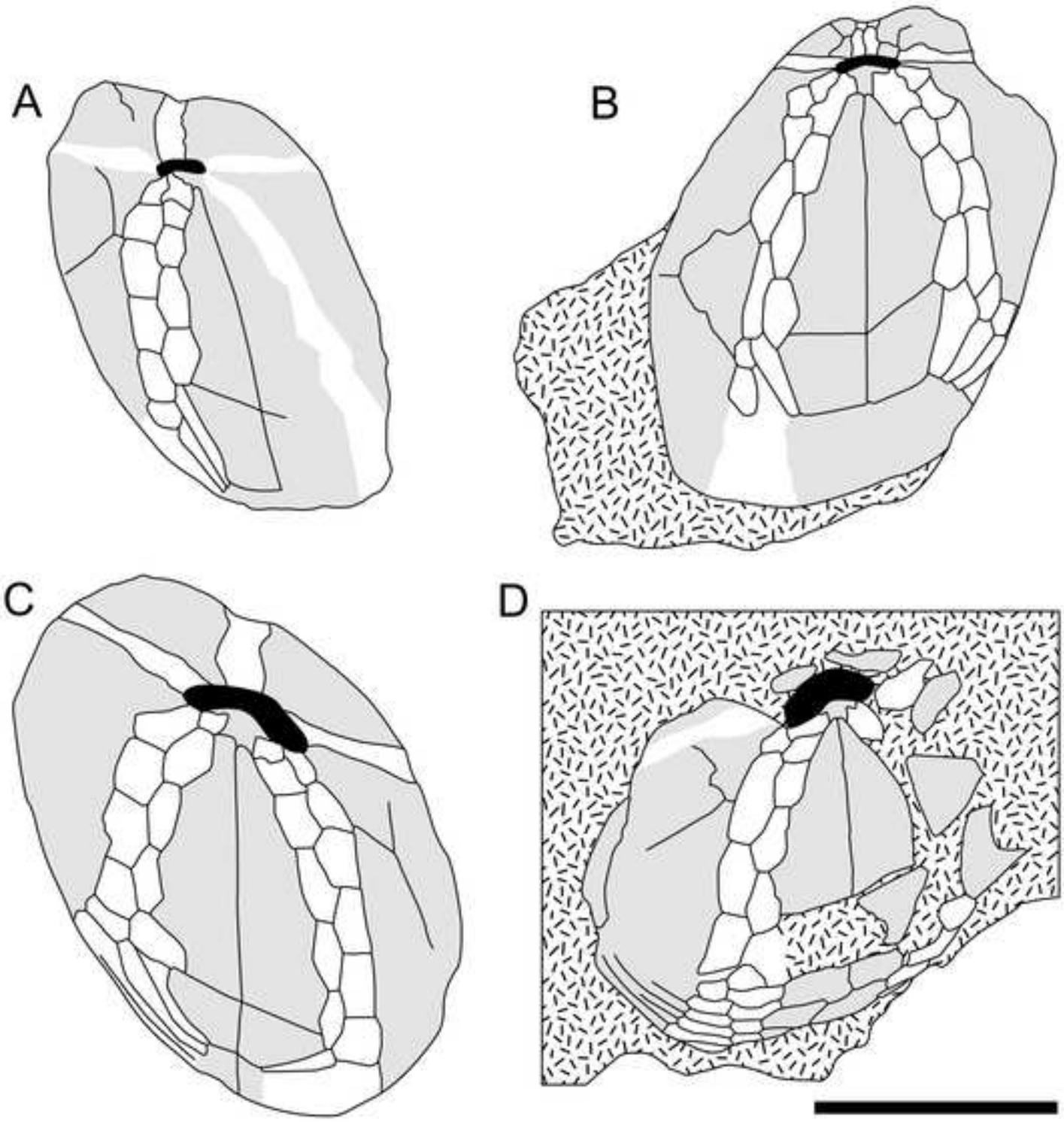

Figure 9

Click here to access/download;Figure;Figure 9 OK.tif

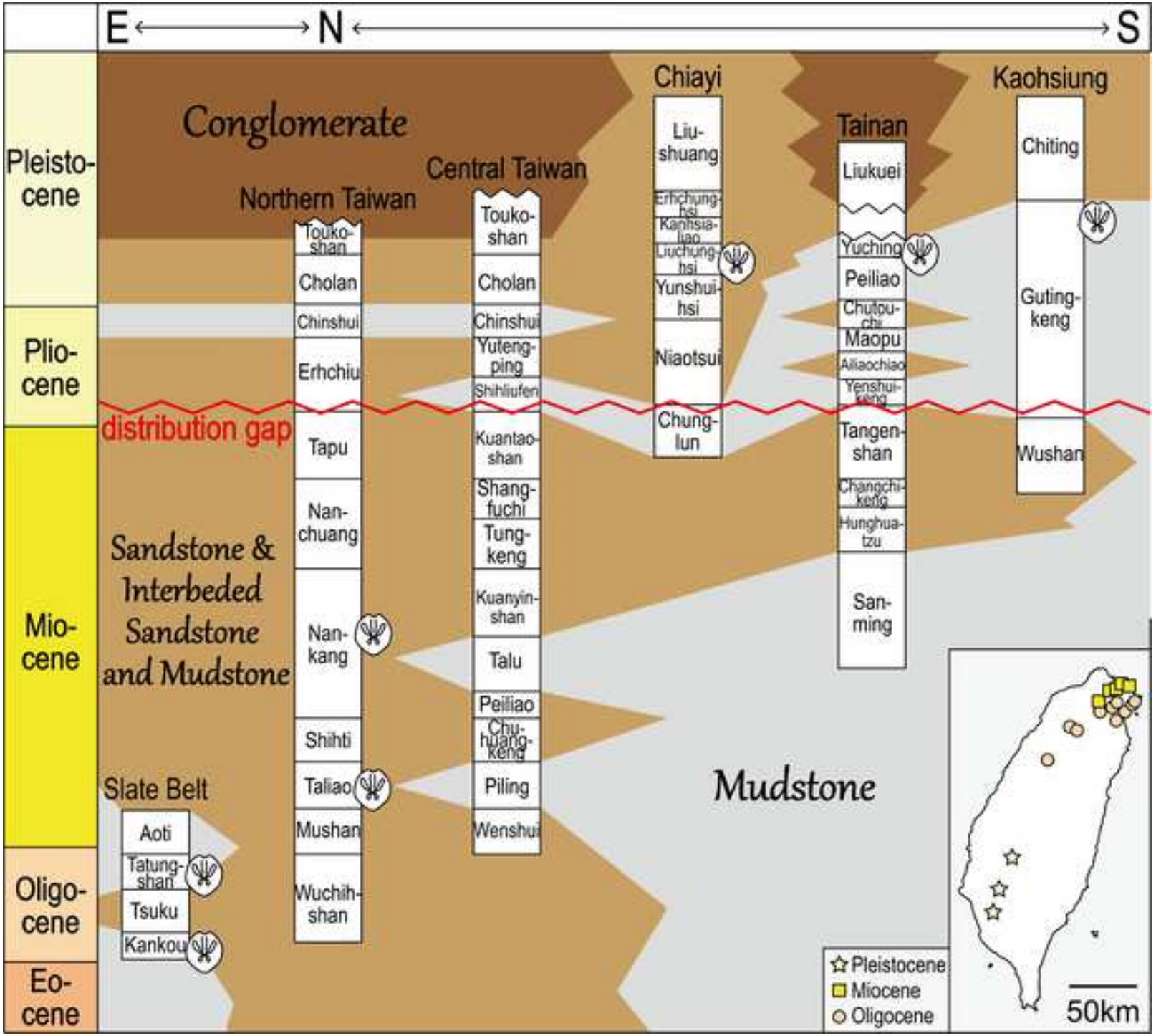

Figure 10

Click here to access/download;Figure;Figure 10 OK.tif

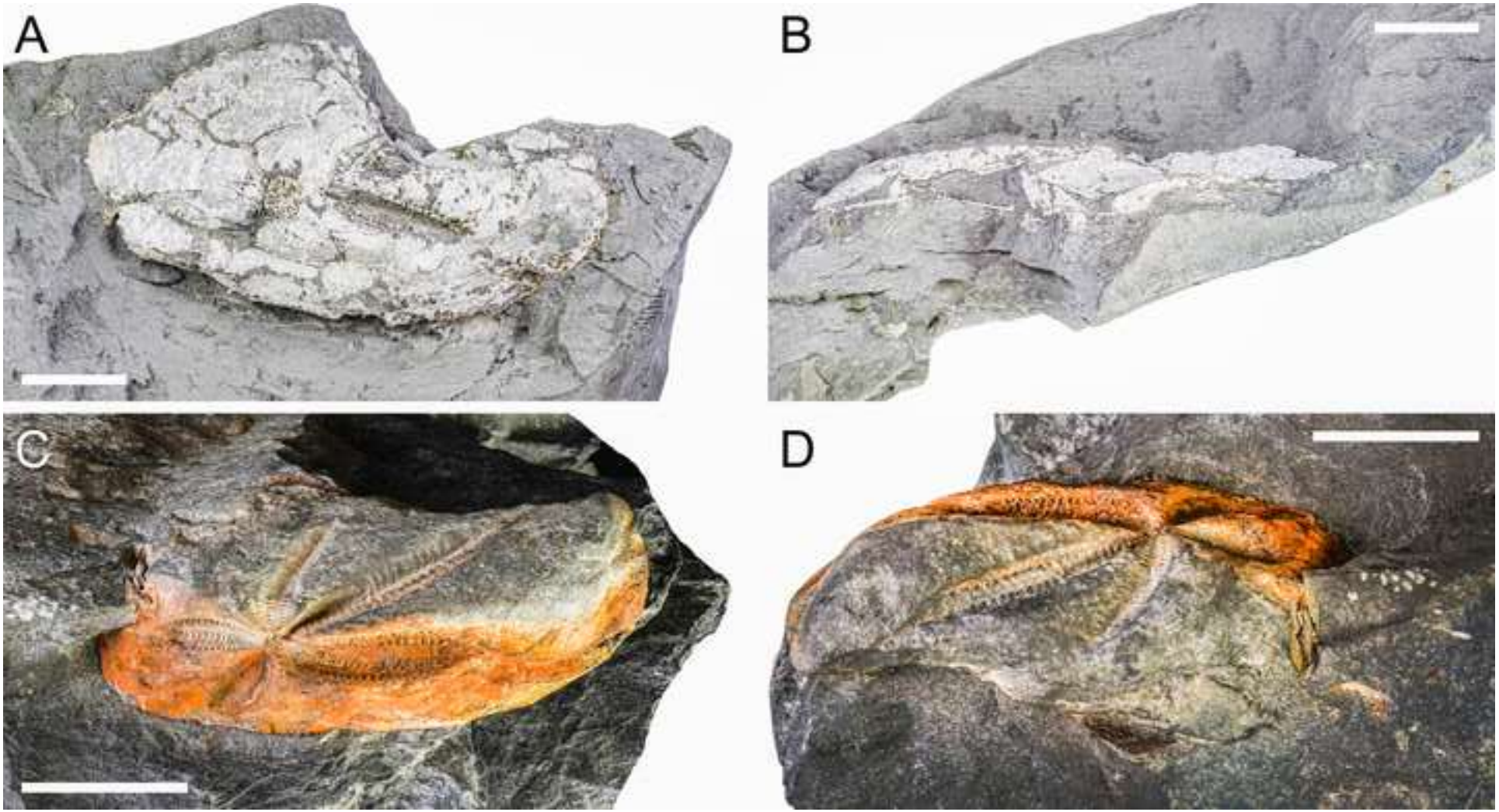

Table 1.

Type	Spines	Position	Function
A	Flattened	Plastron	Locomotion
B	Medium-length, lateral	Adjacent to and outside posterior ambulacrum	Moving sand
C	Short	Around mouth	Feeding
D	Short, lateral	Test margins	Maintaining burrow walls
E	Short	Anterior margin of test	Scraping material from front burrow wall
F	Long	Adjacent to sides of petals	Forming protective arches over petals
G	Long	Aboral side	Building respiratory funnel
H	Tufts of long spines	Subanal fascioles	Building sanitary tube

Table 2.

Species	Locality	Age	Formation	References
Schizaster taiwanicus	Dahu, Hsinchu County Jianshih, Hsinchu County Pinglin, New Taipei City Wulai, New Taipei City Xindian, New Taipei City Daxi, Yilan County Nan'ao, Yilan County Toucheng, Yilan County Waiao, Yilan County	Oligocene	Tatungshan Fm. (Slate Belt)	Tokunaga (1903) Nisiyama (1933) Hayasaka (1948b) Cheng and Wang (1981)
Schizaster sp. 1	Dashehu, New Taipei City Xindian, New Taipei City	Oligocene	Kankou Fm. (Slate Belt)	Hayasaka (1948b)
Schizaster sp. 2	Badouzi, Keelung City	Miocene	Taliao Fm.	Jiang (unpublished data)
Schizaster taiwanicus	Nuannuan, Keelung City Ruifang, New Taipei City Xindian, New Taipei City Xizhi, New Taipei City	Miocene	Nangang Fm.	Cheng and Wang (1981) Huang (2011)
Schizaster sp. 3	Xindian, New Taipei City	Miocene	Nangang Fm.	Cheng and Wang (1981)
Schizaster (*Ova*) sp. 4	Yujing, Tainan City	Early Pleistocene	Yujing Shale	Chuang (2020)
Schizaster (*Ova*) *lacunosus*	Niupu, Chiayi County	Early Pleistocene	Liuchunghsi Fm.	Huang (2011)
Schizaster sp. *5*	Tianliao, Kaohsiung City	Early Pleistocene	Gutingkeng Fm.	This study
Brissopsis sp. 1	Keelung City	Oligocene	Kankou Fm. (Slate Belt)	Nisiyama (1968)
Brissopsis japonica	Xindian, New Taipei City	Miocene	Nangang Fm.	Cheng and Wang (1981)
Brissopsis luzonica	Yujing, Tainan City	Pleistocene	Yujing Shale	Chuang (2020)
	Longgang, Miaoli County		Toukoshan Fm.	Huang (2011)
Brissopsis sp. 2	Tianliao, Kaohsiung City	Early Pleistocene	Gutingkeng Fm.	This study

Appendix A